

Supporting information.

Chemical synthesis.

For the synthesis of 3-Hydroxy-2-isopropyl-3-phenyl-1-isoindolinone, 2-benzoylbenzoic acid (1 equiv.) was dissolved in DCM while cooling in a round bottom flask. After mixing the solution for 5 min, triethylamine (3 equiv.) and propan-2-amine (1.2 equiv.) were added in cooling conditions. Then, stirring of the mixture was performed for 20 min before 2,4,6- tripropyl-1,3,5,2,4,6-trioxatriphosphinane 2,4,6-trioxide (1.2 equiv.) were added to the reaction mixture at once under cooling. After the reaction resulted complete according to TLC analysis (approximately after 3 h of stirring), DCM was added to dilute the mixture before a washing step with HCl (1 M solu., 10 ml x 3). Afterwards, ethyl acetate (20 ml x 3) was employed for the organic extraction and a 2M solution of NaOH was used for the washing of the combined organic layers followed by water and brine and drying over Na₂SO₄. Ultimately, evaporation of the solvent was performed under reduced pressure conditions.

The resulting crystals had ca. 98% purity (determined by ¹H NMR).

Thermal analysis of the flow reactor.



Figure S1. Thermal images of the a) two water baths at different temperatures b) the connecting tube entering the cold bath and c) the tube leaving the cold bath.

The thermal profile along the tubular reactors was investigated by pointing the thermal camera to the connecting tube which was not totally immersed in the water baths. Figure S1a shows the overall set-up configuration comprising of two thermal zones with the tubular reactors passing through them in a loop fashion. In the case of forced cooling with the cold bath the solution leaving the hot zone cools gradually in the section exposed to ambient air and then it cools almost instantaneously once entering the cold bath (Figure S1b). Then, no thermal gradient is observed and, regardless of the length of the tube inside the low temperature zone, the temperature of the solution is practically maintained constant until the exit from the water bath (Figure S1c). After that the solution passes through the peristaltic pump before entering again the hot bath without major thermal variations due to the similar temperature conditions between the cold bath and the ambient air.

On the other hand, for the experiments with 15 s and 30 s residence time the crystallization phase was performed under natural convection cooling due to the limited length of the reactor. Figure S2 displays how the solution recirculating in the loop system cools rapidly after leaving the hot bath even though the lowest temperature values attained are not comparable with the ones reached in the cold bath.

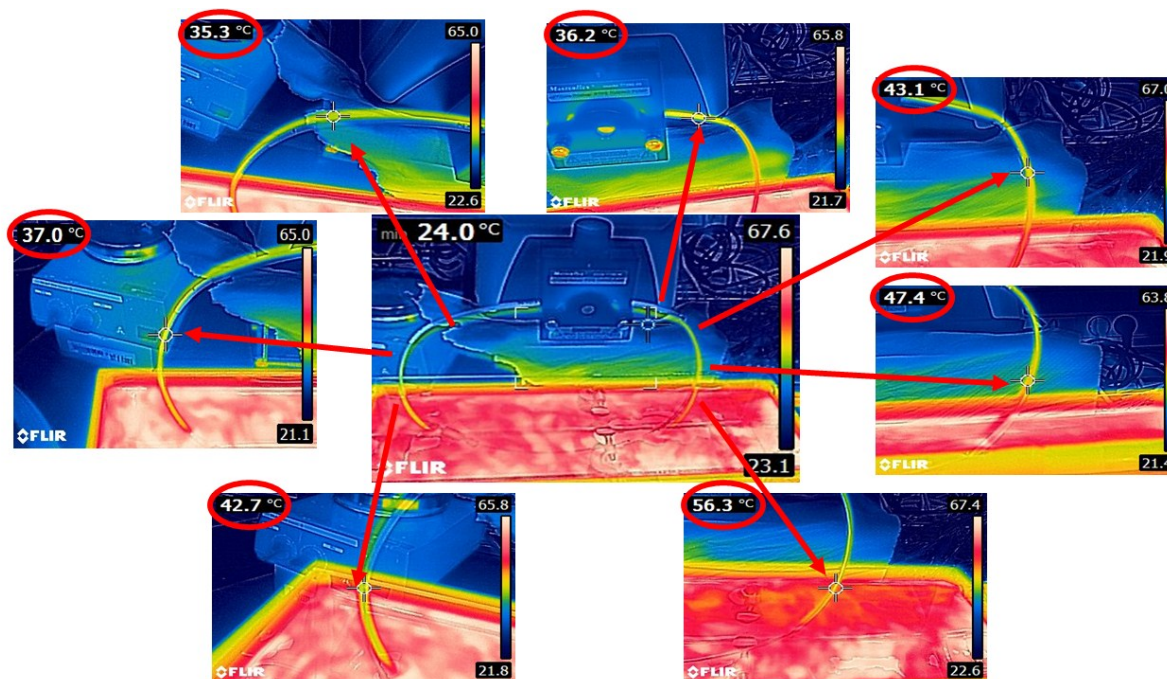


Figure S2. Thermal analysis of set-up with natural convection cooling.

Isothermal conditions.

The extreme case of short residence time is the complete absence of thermal oscillations which can be achieved by placing the whole reactor in the cold thermal bath at 25 °C. This process conditions lead to no deracemization as the suspension prepared with initial 20% enantiomeric excess of the dry crystals (enantiomeric purity of 60%) attains only 36% excess (68% purity) after 100 equivalent cycles which is in line with theoretical equimolar dissolution at the operating low temperature.

Effect of suspension flow rate.

The effect of suspension flow rate was investigated by doubling the reactor length and the flow rate at the same time so to maintain the same residence time per cycle. Therefore, two reactors comprising of 20 s dissolution time and 40 s crystallization time are compared in Figure S3 where it is apparent that under these conditions no substantial effect in deracemization rate can be observed when increasing the

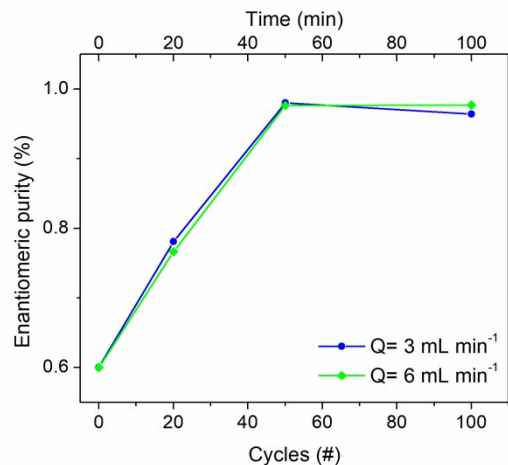


Figure S3. Deracemization rate of processes run with the same residence time per cycle but different suspension flow rate.

suspension flow rate from 3 to 6 mL min⁻¹. Further experiments could not be performed as at lower flow rate the flow regime of the suspension would be affected so to cause the crystals to settle at the bottom of the tube and at higher values of flow rate the particles would be pushed together and ultimately result in clogging of the reactor.

SEM images.

A visual inspection of the particles employed in the process was taken via SEM analysis in order to observe both the particles before the application of thermal cycles and at the end of the deracemization process.

Figure S4 displays the chiral particles before and after the runs for 20 and 100 cycles at 2 min residence time per cycle. The presence of small fines among the initial particles is due to the fact that the initial enantiomeric excess was attained by mixing racemic crystals with enantiopure ones obtained from previous deracemization processes via thermal cycles that induce substantial size reduction of the crystal population.

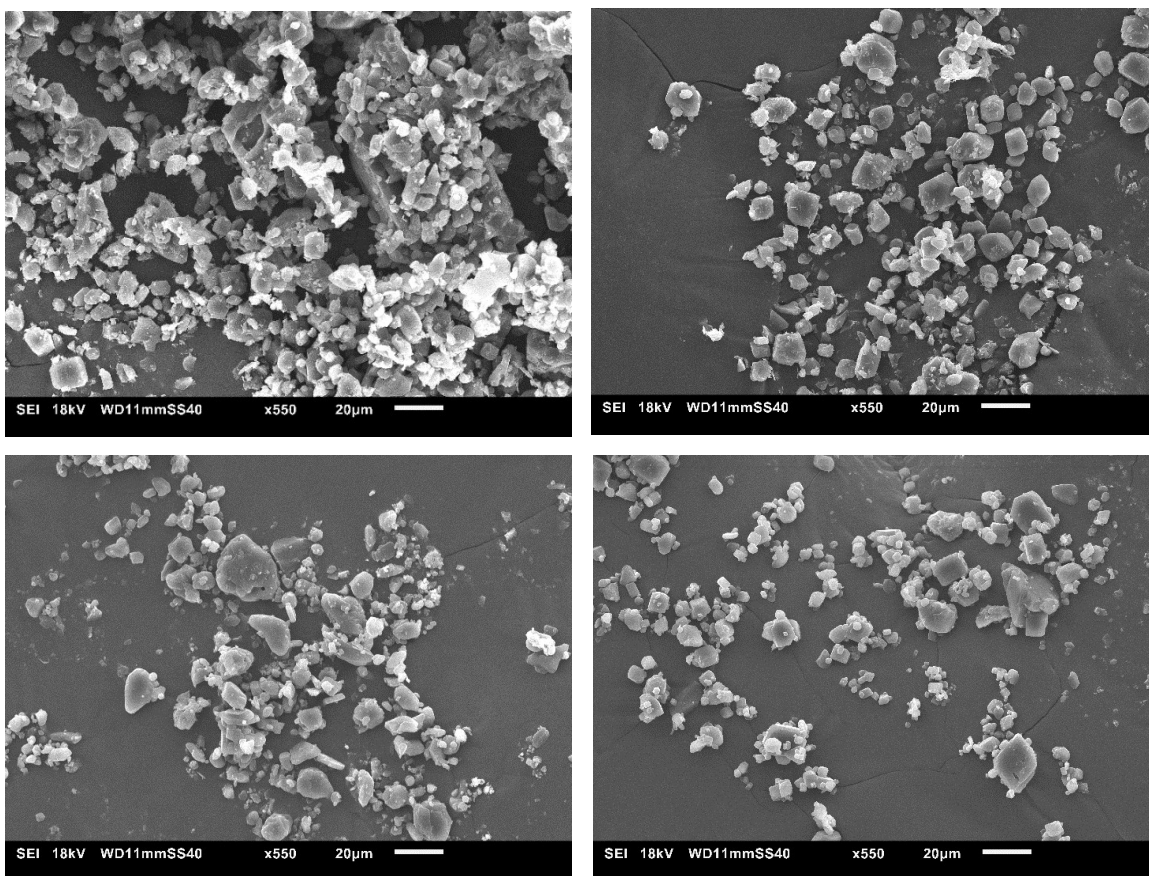


Figure S4. SEM photographs of the chiral particles employed before (top left) and after (top right) the run for 20 cycles and before (bottom left) and after (bottom right) the run for 100 cycles in the reactor featuring 2 min residence time per cycle.

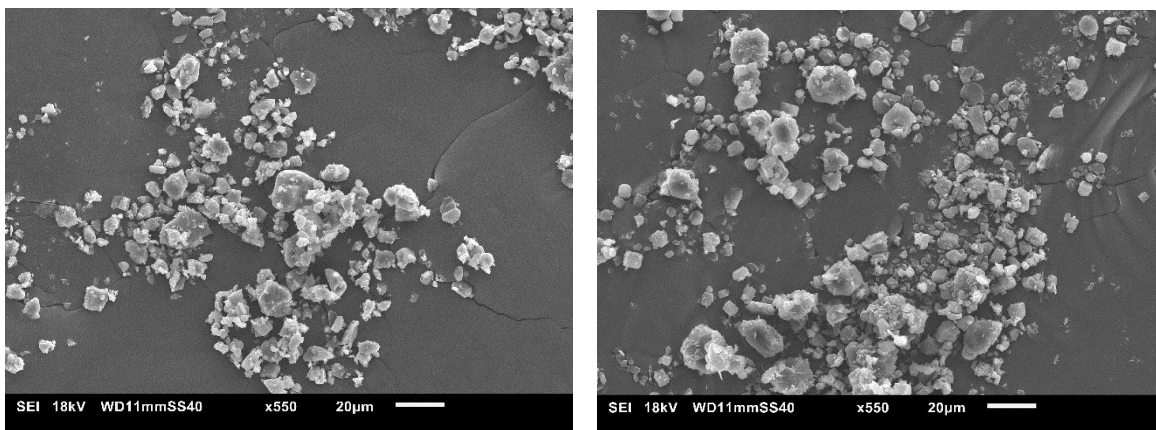


Figure S5. SEM photographs of the initial (left) and final (right) particles employed in the deracemization process at high flow rate (6 mL min^{-1}) for 100 cycles.

On the other hand, the big size span among the final particles can be seen as a proof that at the high level of supersaturation ($S_i = 2$) achieved in the process secondary nucleation plays a central role in the crystallization phase and even if smaller particles would preferentially dissolve in the hot temperature stage, no clear fines removal can be observed in this case as it is in other applications of temperature cycling.

A similar trend is observed for the processes run with high flow rate (Figure S5) and high suspension density (Figure S6) in which the big particles do not seem to increase in size while very small crystals are retrieved at the end of the process.

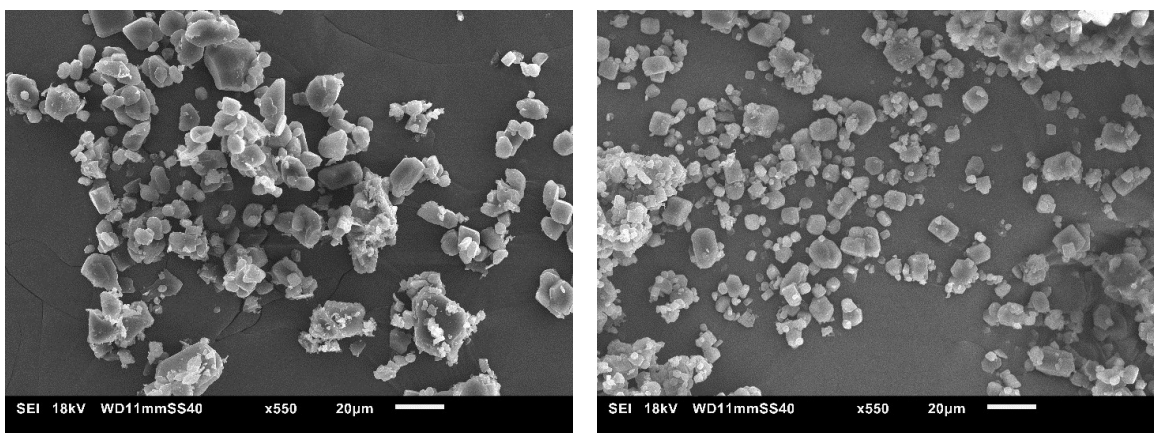


Figure S6. SEM images of the crystals employed in the deracemization experiment at high suspension density ($78.8 \text{ mg L}_{\text{solvent}}^{-1}$): initial particles (left) and process outcome (right).

